Research Article | Vol. 24, No. 15 | 25 Jul 2016 | OPTICS EXPRESS 16815

Optics EXPRESS

Electrically tunable transmission of gold binary-grating metasurfaces integrated with liquid crystals

KUO-PING CHEN,[1,*] SHI-CHENG YE,[2] CHI-YIN YANG,[1] ZONG-HAN YANG,[1] WEI LEE,[1] AND MAO-GUO SUN[1]

[1]*Institute of Imaging and Biomedical Photonics, National Chiao Tung University, 301 Gaofa 3rd Road, Tainan, Taiwan*
[2]*Institute of Lighting and Energy Photonics, National Chiao Tung University, 301 Gaofa 3rd Road, Tainan, Taiwan*
[*]*kpchen@nctu.edu.tw*

Abstract: Planar photonics using metasurfaces is of great interest because a metasurface can control the flow of light beyond that attainable with natural materials. The resonance wavelength of a binary-grating metasurface is adjustable by changing the width and thickness of the nanostructure. We propose a novel combination of nematic liquid crystals and a binary-grating metasurface with which the diffraction efficiency can be controlled by adjusting the applied voltage.

OCIS codes: (250.5403) Plasmonics; (160.3918) Metamaterials; (230.3720) Liquid-crystal devices.

References and links

1. T. C. Choy, *Effective Medium Theory: Principles and Applications* (Oxford University, 1999).
2. M. Tyboroski, N. Anderson, and R. Camley, "An effective medium study of surface plasmon polaritons in nanostructured gratings using attenuated total reflection," J. Appl. Phys. **115**(1), 013104 (2014).
3. P. Shekhar, J. Atkinson, and Z. Jacob, "Hyperbolic metamaterials: fundamentals and applications," Nano Converge. **1**(1), 1–17 (2014).
4. N. Yu, P. Genevet, M. A. Kats, F. Aieta, J.-P. Tetienne, F. Capasso, and Z. Gaburro, "Light propagation with phase discontinuities: generalized laws of reflection and refraction," Science **334**(6054), 333–337 (2011).
5. H. Tao, A. C. Strikwerda, K. Fan, W. J. Padilla, X. Zhang, and R. D. Averitt, "Reconfigurable terahertz metamaterials," Phys. Rev. Lett. **103**(14), 147401 (2009).
6. I. M. Pryce, K. Aydin, Y. A. Kelaita, R. M. Briggs, and H. A. Atwater, "Highly strained compliant optical metamaterials with large frequency tunability," Nano Lett. **10**(10), 4222–4227 (2010).
7. J.-Y. Ou, E. Plum, J. Zhang, and N. I. Zheludev, "An electromechanically reconfigurable plasmonic metamaterial operating in the near-infrared," Nat. Nanotechnol. **8**(4), 252–255 (2013).
8. M. A. Kats, R. Blanchard, P. Genevet, Z. Yang, M. M. Qazilbash, D. N. Basov, S. Ramanathan, and F. Capasso, "Thermal tuning of mid-infrared plasmonic antenna arrays using a phase change material," Opt. Lett. **38**(3), 368–370 (2013).
9. F. Huang and J. J. Baumberg, "Actively tuned plasmons on elastomerically driven Au nanoparticle dimers," Nano Lett. **10**(5), 1787–1792 (2010).
10. M. Abb, P. Albella, J. Aizpurua, and O. L. Muskens, "All-optical control of a single plasmonic nanoantenna-ITO hybrid," Nano Lett. **11**(6), 2457–2463 (2011).
11. Y. Yao, M. A. Kats, P. Genevet, N. Yu, Y. Song, J. Kong, and F. Capasso, "Broad electrical tuning of graphene-loaded plasmonic antennas," Nano Lett. **13**(3), 1257–1264 (2013).
12. Y. Yao, R. Shankar, M. A. Kats, Y. Song, J. Kong, M. Loncar, and F. Capasso, "Electrically tunable metasurface perfect absorbers for ultrathin mid-infrared optical modulators," Nano Lett. **14**(11), 6526–6532 (2014).
13. A. Karvounis, B. Gholipour, K. F. MacDonald, and N. I. Zheludev, "All-dielectric phase-change reconfigurable metasurface," arXiv preprint arXiv:1604.01330 (2016).
14. Y.-W. Huang, H. W. H. Lee, R. Sokhoyan, R. Pala, K. Thyagarajan, S. Han, D. P. Tsai, and H. A. Atwater, "Gate-tunable conducting oxide metasurfaces," arXiv preprint arXiv:1511.09380 (2015).
15. Y.-H. Chen, K.-P. Chen, M.-H. Shih, and C.-Y. Chang, "Observation of the high-sensitivity plasmonic dipolar antibonding mode of gold nanoantennas in evanescent waves," Appl. Phys. Lett. **105**(3), 031117 (2014).
16. Z.-Y. Yang and K.-P. Chen, "Effective absorption enhancement in dielectric thin-films with embedded paired-strips gold nanoantennas," Opt. Express **22**(11), 12737–12749 (2014).
17. M.-S. L. Lee, P. Lalanne, J.-C. Rodier, and E. Cambril, "Wide-field-angle behavior of blazed-binary gratings in the resonance domain," Opt. Lett. **25**(23), 1690–1692 (2000).

#263570 http://dx.doi.org/10.1364/OE.24.016815
Journal © 2016 Received 20 Apr 2016; revised 1 Jul 2016; accepted 8 Jul 2016; published 18 Jul 2016

Optics EXPRESS

18. J. M. Miller, M. R. Taghizadeh, J. Turunen, and N. Ross, "Multilevel-grating array generators: fabrication error analysis and experiments," Appl. Opt. **32**(14), 2519–2525 (1993).
19. T. Roy, A. E. Nikolaenko, and E. T. Rogers, "A meta-diffraction-grating for visible light," J. Opt. **15**(8), 085101 (2013).
20. Z. Peng, D. A. Fattal, A. Faraon, M. Fiorentino, J. Li, and R. G. Beausoleil, "Reflective silicon binary diffraction grating for visible wavelengths," Opt. Lett. **36**(8), 1515–1517 (2011).
21. M. Collischon, H. Haidner, P. Kipfer, A. Lang, J. T. Sheridan, J. Schwider, N. Streibl, and J. Lindolf, "Binary blazed reflection gratings," Appl. Opt. **33**(16), 3572–3577 (1994).
22. A. Pors, O. Albrektsen, I. P. Radko, and S. I. Bozhevolnyi, "Gap plasmon-based metasurfaces for total control of reflected light," Sci. Rep. **3**, 2155 (2013).
23. M. W. Farn, "Binary gratings with increased efficiency," Appl. Opt. **31**(22), 4453–4458 (1992).
24. B. K. Singh and A. C. Hillier, "Surface plasmon resonance enhanced transmission of light through gold-coated diffraction gratings," Anal. Chem. **80**(10), 3803–3810 (2008).
25. W.-H. Yeh, J. W. Petefish, and A. C. Hillier, "Diffraction-based tracking of surface plasmon resonance enhanced transmission through a gold-coated grating," Anal. Chem. **83**(15), 6047–6053 (2011).
26. J. A. Davis, K. O. Valadéz, and D. M. Cottrell, "Encoding amplitude and phase information onto a binary phase-only spatial light modulator," Appl. Opt. **42**(11), 2003–2008 (2003).
27. G. Meltz, W. W. Morey, and W. H. Glenn, "Formation of Bragg gratings in optical fibers by a transverse holographic method," Opt. Lett. **14**(15), 823–825 (1989).
28. P. B. Johnson and R.-W. Christy, "Optical constants of the noble metals," Phys. Rev. B **6**(12), 4370–4379 (1972).
29. M. Moharam, T. Gaylord, D. A. Pommet, and E. B. Grann, "Stable implementation of the rigorous coupled-wave analysis for surface-relief gratings: enhanced transmittance matrix approach," J. Opt. Soc. Am. A **12**(5), 1077–1086 (1995).
30. L. Li, "Use of Fourier series in the analysis of discontinuous periodic structures," J. Opt. Soc. Am. A **13**(9), 1870–1876 (1996).
31. P. Lalanne and G. M. Morris, "Highly improved convergence of the coupled-wave method for TM polarization," J. Opt. Soc. Am. A **13**(4), 779–784 (1996).
32. S.-H. Sun, M.-J. Lee, Y.-H. Lee, W. Lee, X. Song, and C.-Y. Chen, "Immunoassays for the cancer biomarker CA125 based on a large-birefringence nematic liquid-crystal mixture," Biomed. Opt. Express **6**(1), 245–256 (2014).

1. Introduction

Plasmonic metasurfaces are optical devices composed of subwavelength ridges distributed with a period that controls the phase of light. For planar photonics devices, a metasurface can be used to direct the wavefront of the propagating light by using a discontinuous phase shift. In general, nanostructured film is an effective medium when the period of the structure is smaller than the wavelength of the light to be directed [1–3]. The plasmonic binary grating has received considerable attention recently because it was like two-dimensional metasurface, a subwavelength structure about 1/30 of a wavelength thick, can generate high-efficiency diffraction.

When the phase gradient $\nabla\phi$ in the surface of the material is considered, the generalized Snell's law equations are [4],

$$n_t \sin\theta_t - n_i \sin\theta_i = \frac{\lambda\nabla\phi}{2\pi}, \tag{1}$$

$$\sin\theta_r - \sin\theta_i = \frac{\lambda\nabla\phi}{2\pi n_i}, \tag{2}$$

where θ_i, θ_t, and θ_r are the angles of incidence, refraction, and reflection, respectively. Electromagnetic (EM) waves of wavelength λ propagate from the incident medium with refractive index n_i, to the substrate medium, with refractive index n_t. When $\nabla\phi = 0$ along the interface between the metal and the dielectric, Eqs. (1) and (2) are reduced to the traditional Snell's law equations. According to Eq. (1), the direction of the refracted light can be controlled with changes in $\nabla\phi$.

The development of metasurfaces with reconfigurable or tunable optical responses would be important technology to achieve reconfigurable flat optics and optoelectronics [5–7]. There

Optics EXPRESS

have been researches in developing tuning methods of metamaterials depends on temperature [8], stress [9], nonlinear optics [10], and electrical signals [11]. In order to make compact flat optoelectronics devices, electrical tuning methods would be most promising. Several different materials have been applied to the reconfigurable metasurfaces, like graphene [11, 12], phase change materials [8, 13], transparent conducting oxide [10, 14], etc. However, those materials are expensive and not easy to fabricate. In this work, the liquid crystal (LC) is proposed to reconfigurable metasurface. The advantage of liquid crystal would be its low cost, and easy in fabrication.

There are several advantages of using a binary grating as a two-dimensional metasurface to control the flow of light. First, a binary grating could act as an aligning layer to align LC molecules, but nanobricks structures cannot [15–17]. Second, it is easier to fabricate a binary grating than a multilevel grating or graded-index gratings [18]. Third, the subwavelength thicknesses of metasurface can be applied to the thinner optical devices [19]. Although the thickness of a binary grating is small compared with the incident wavelength, it can still manipulate both the amplitude and the phase of light when it operates at the plasmonic resonance wavelength [20, 21]. A plasmonic binary grating consists of a monolayer of gold nanostrips that are capable of controlling the wavefront of light. Here, we present our design for a binary grating and its integration with a high-birefringence LC to control diffraction efficiency. Binary gratings metasurfaces have excellent potential for use as high-efficiency light-steering components [22, 23], switchable surface plasmon couplers [24, 25], and in high-resolution holography [26, 27].

2. Materials, grating design, and sample fabrication

Figure 1(a) compares four types of gratings with different gradient phase modulation. Although blazed, multilevel, and graded index gratings provide ideal phase profiles, they are difficult to fabricate, so we investigated the binary grating as a two-dimensional metasurface. Figure 1(b) shows a supercell of a binary-grating metasurface consisting of a Au nanostructure of varying widths and a 2880 nm period on a glass substrate. The dielectric function of Au was taken from the database of Johnson and Christy [28]. This binary grating was constructed by sequentially placing Au nanostrips, with a center-to-center distance of 240 nm, in a supercell. The grating widths were 50, 50, 70, 70, 90, 90, 110, 110, 130, 130, 150, and 150 nm. The + 1 diffraction angle was 13.1°. Figure 1(c) shows the transmittance for orders 0, + 1, and –1, revealing the resonance wavelength at ~650 nm. The finite element method (FEM) software package COMSOL Multiphysics 4.3b was used to design the binary gratings [29–31].

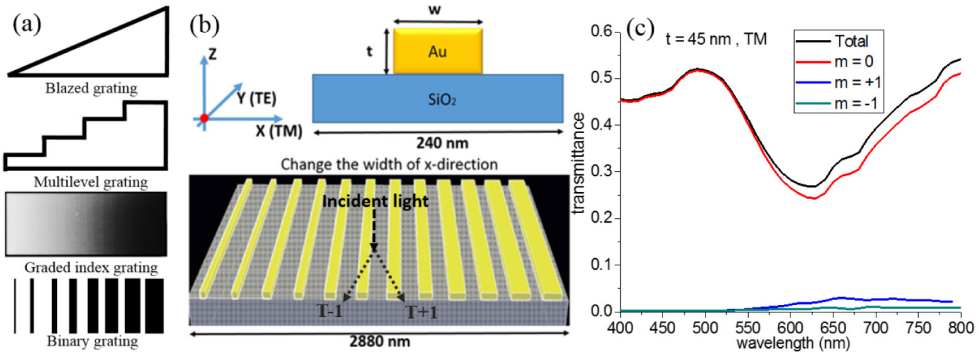

Fig. 1. (a) Comparison of different gratings. (b) Schematic of a supercell of a binary grating comprising a Au grating of different widths and a 2880 nm period on a substrate of ITO glass surrounded by air. (c) The simulated transmission spectra for a 45 nm thick binary grating in TM polarization, where $m = 0$, $m = +1$, and $m = -1$ are the diffraction orders.

Optics EXPRESS

The binary-grating metasurface samples were fabricated by E-beam lithography (EBL). First, the substrate was spin-coated with positive electron beam resist PMMA (A4 950K) at a spinning speed of 8000 rpm for 50 s. Followed by soft baking at 180 °C for 90 s. Second, the PMMA was patterned using EBL (ELIONIX ELS-7500EX) with the exposure dose of 270 μC/cm^2 and the beam voltage is 50 kV. The sample was then developed using MIBK:IPA (1:3) development for 30 s. Finally, electron beam deposition was used to deposit 5 nm and 45 nm Ti and Au thin films with the evaporation rate as 0.5 and 1 Å/s, respectively. The undefined PMMA and excess metal were stripped using acetone. Figure 2(a) is a scanning electron microscope (SEM) image of a well-defined Au binary-grating metasurface, with grating widths ranging from 50 to 150 nm and a period P of 2880 nm. Figure 2(b) is a three-dimensional (3D) topographical image of the grating obtained using atomic force microscopy (AFM), and Fig. 2(c) is a topographical chart of the cross section that shows the grating to be about 45 nm thick.

The LC material used in this study is a eutectic nematic mixture designated HTW [32]. It has a broad nematic temperature range from < –30 °C to 95 °C, and has high birefringence (Δn = 0.333 at a wavelength of 589.3 nm and a temperature of 20 °C) and reasonably large dielectric anisotropy ($\Delta\varepsilon$ = + 10.4 at 1 kHz and 25 °C). The wide nematic range warrants the stability of mesogenic properties, and the high birefringence and large dielectric anisotropy favor wider spectral tunability and lower operation voltage, respectively. The substrate with the nanostructured surface serves as the bottom substrate for the LC cell. The other substrate is a typical indium–tin-oxide (ITO)-coated glass slide spin-coated with a polyimide layer for LC's planar alignment and successively treated with mechanical buffing along the x-direction to impose a unidirectional orientation of the LC molecules. The assembled empty cell has a thickness (i.e., cell gap) of *ca.* 10 μm, as determined by silica spacers. It was filled with the nematic LC HTW by capillary action at room temperature.

Figure 2(d) shows the schematic of binary grating metasurfaces combined with nematic LC as reconfigurable devices which could be tuned by electric signal. Making use of the characteristics of nematic LC which can achieve polarization change and be able to tune the diffraction efficiency in binary gratings metasurfaces.

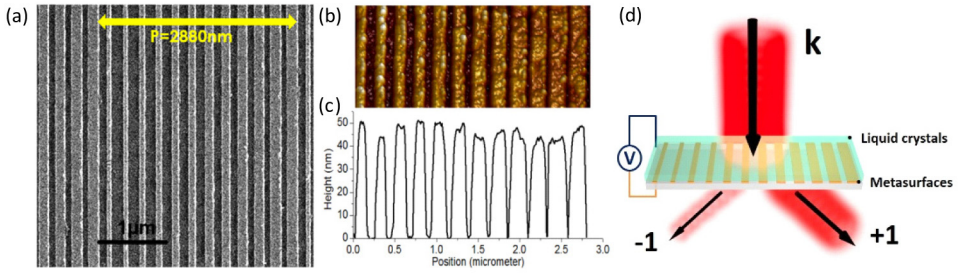

Fig. 2. (a) SEM image of a Au binary grating (t = 45 nm) with grating widths of 50, 50, 70, 70, 90, 90, 110, 110, 130, 130, 150, and 150 nm. (b) 3D AFM topographical image. (c) Cross-sectional topographical chart showing that the binary grating is about 45 nm thick. (d) Schematic of a reconfigurable binary grating metasurface as part of a LC cell.

3. Results and discussion

Figures 3(a) and 3(b) show the ratio of diffraction orders m = + 1 to m = –1 as a function of wavelength in TM and TE polarizations, respectively. In TM polarization, the diffraction ratio has a strong dependence on wavelength. In the 450–560 nm wavelength range, the ratio is equal to 1 because the Au plasmonic resonance wavelength does not fall in that range. The ratio increases in the 560–800 nm range and reaches maximum at ~650 nm. This result corresponds well with the transmittance spectra in TM polarization as shown in Fig. 1(c). On the other hand, in TE polarization, the diffraction ratio is ~0.5 and does not change significantly as the wavelength increases [Fig. 3(b)]. Figure 4(a) shows the schematic of the

Optics EXPRESS

diffraction measurement setup. Red and green solid-state lasers were used to measure the diffraction efficiency of the binary grating at wavelengths of 653 nm and also 533 nm. The simulation and experimental results, obtained using a laser power meter (Ophir Optronics Solutions), show good agreement with little deviation. The deviation between simulation and experimental results could be due to the imperfection in samples fabrication, roughness and sidewall angles of the gratings.

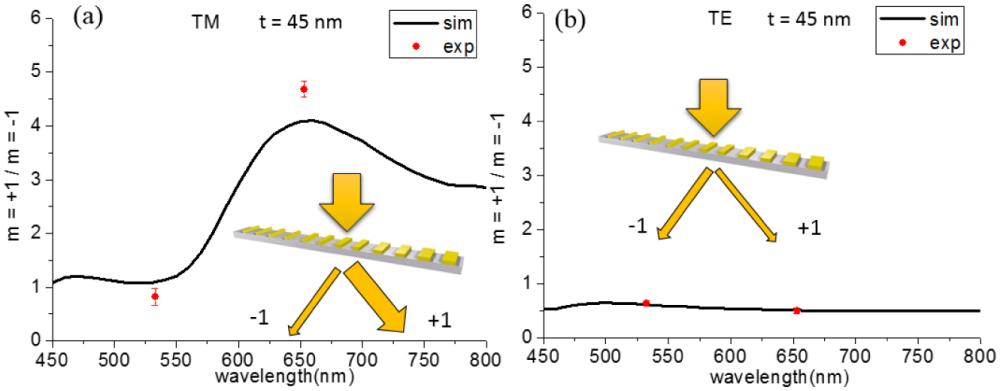

Fig. 3. Diffraction ratio (m = + 1/m = –1) vs. wavelength in (a) TM and (b) TE polarization.

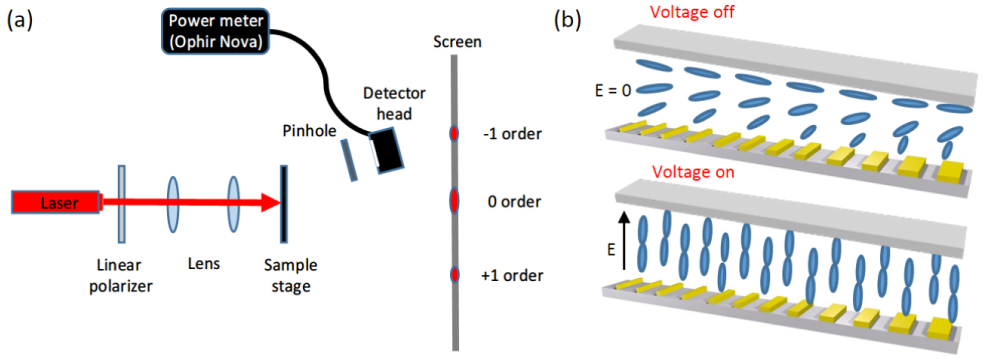

Fig. 4. (a) Schematic of the diffraction measurement system. (b) Schematic of binary gratings combined with nematic LC when the voltage is on and off.

To tune the anomalous diffraction ratio, we used the high-birefringence nematic LC HTW to control the polarization of the incident light. The binary grating on the bottom substrate is perpendicular to the alignment of the LC on the top electrode. When the incident light is in TM polarization and the voltage is turned off, the LC causes the polarization state of the light to rotate 90°. In other words, TM polarization changes to TE polarization because of the twisted alignment of the LC bulk and the metasurface function is off. On the other hand, when the voltage is turned on, the metasurface function is on. Figure 4(b) shows the scheme of the binary grating combined with nematic LC.

The LC used in our study has high optical anisotropy. At 589 nm and 20 °C, the LC possesses birefringence Δn of 0.333 and refractive indices n_e and n_o of 1.851 and 1.518, respectively. The top and bottom electrodes permit AC voltage (at 1 kHz) to be applied across

Optics EXPRESS

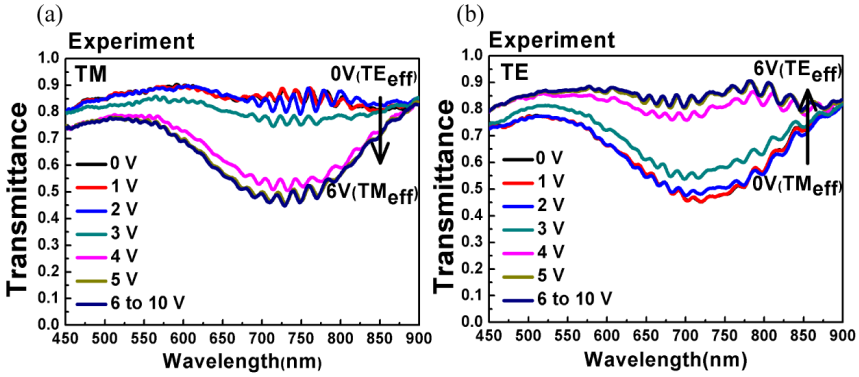

Fig. 5. (a) Transmittance spectra with nematic liquid crystals as increase of voltage in TM polarization of incident light. (b) Transmission spectrum with nematic liquid crystals as increase of voltage in TE polarization of incident light. The little fringes in spectra are due to two substrate-LC boundaries caused light interference.

the cell thickness. Figure 5(a) shows the transmittance spectra of the LC cell at various voltages (V) in TM polarization of incident light. When $V = 0$ to 2 V_{rms}, the voltages are too small to reorient the LC molecules perpendicular to the substrate. Therefore, the incident light on the binary grating can be considered as TE polarization in the voltage-on state. When $V > 3$ V_{rms}, the LC establishes a configuration where the nematic director is perpendicular to the substrate so that the resonance dip appears; it means that the incident light on the binary grating can be considered as TM polarization in the voltage-on state. Figure 5(b) shows the transmittance spectra of the cell in TE polarization of incident light. Similarly, the LC is reoriented vertically when $V > 6$ V_{rms}. Therefore, the effective light incident on the binary grating can be considered as TE polarization in the voltage-on state.

Figure 6(a) shows how changing the applied voltage affects the diffraction intensity in $m = + 1$ and -1. By increasing the voltage, the diffraction intensity remains stable in $m = -1$ but increases in $m = + 1$. The diffraction ratio also increases until the voltage reaches 6 V_{rms}, as shown in Fig. 6(b), because when the voltage is applied, the LC molecules no longer "rotate" the polarization of the incident light. The images in Fig. 6(c) of the laser spots for $m = + 1$ and -1 with nematic LC present were obtained by applying different voltages in TM polarization, which manifest that our device can control the flow of light.

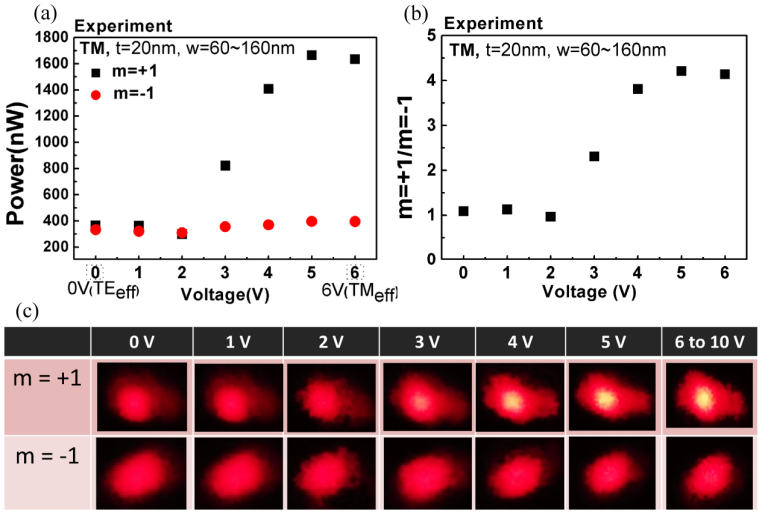

Fig. 6. (a) Diffraction efficiency of the binary grating metasurface combined with nematic LC in TM polarization. Diffraction intensity in $m = + 1$ and $m = -1$. (b) Diffraction ratio as a function of voltage. (c) Images of 653 nm laser spots for $m = + 1$ and $m = -1$.

Optics EXPRESS

4. Conclusions

Binary-grating metasurfaces can be used for engineering electromagnetic phases and controlling light propagation. We demonstrated that an electrically tunable metasurface can be realized by combining a binary grating with nematic LCs. Our findings are important for the development of advanced metasurfaces and their future applications in beam-steering, cloaking, and holography.

Acknowledgments

This work was supported by the Ministry of Science and Technology, Taiwan, ROC (MOST 104-2221-E-009-130-MY3 and 104-2112-M-009-008-MY3), and also by "Aiming for the Top University Program" of the National Chiao Tung University and Ministry of Education, Taiwan, R.O.C.